Hindawi Publishing Corporation
International Journal of Microwave Science and Technology
Volume 2012, Article ID 590153, 9 pages
doi:10.1155/2012/590153

Research Article

Performance Comparison of UWB Pulse Modulation Schemes under White Gaussian Noise Channels

O. Abedi and M. C. E. Yagoub

School of Electrical Engineering and Computer Science, University of Ottawa, Ottawa, ON, Canada K1N 6N5

Correspondence should be addressed to M. C. E. Yagoub, myagoub@site.uottawa.ca

Received 31 January 2012; Revised 21 June 2012; Accepted 23 June 2012

Academic Editor: Xianming Qing

In this paper, and for the first time, the performance of various ultra wideband pulse modulation schemes are discussed and compared in terms of narrowband interference robustness, symbol error rate, system complexity, data rate, and maximum transmit power with respect to transceiver distance and channel capacity. The channel model is the UWB IEEE 802.15.3a multipath indoor channel model under additive white Gaussian noise. The transmit power was evaluated by integrating the fifth derivative of the power spectrum density of the Gaussian pulse over the whole bandwidth.

1. Introduction

In ultra wideband (UWB) system design, there are always tradeoffs between maximum transmit distance, data rate, transmit power, and system complexity. Different data modulation schemes such as pulse-position modulation (PPM), pulse-amplitude modulation (PAM), phase-shift keying (PSK), or on-off keying (OOK) have been used in UWB communications with relative success depending on the targeted application [1, 2]. In fact, their performance can significantly vary according to which system parameters are considered such as narrowband interference (NBI) robustness, symbol error rate (SER), system complexity, data rate, or maximum transmit power with respect to transceiver distance and channel capacity. For instance, if minimum complexity is important, then OOK modulation would be the best choice. However, it is very sensitive to noise. On the other side, if interference robustness and power efficiency are the parameters to consider, binary PSK (BPSK) and M-ary PPM (M-PPM) can be the best candidates. Nevertheless, M-PPM deals with multidimensional signals, whereas M-PAM has only one dimension [3, 4].

This topic has been widely discussed in the last decade but most of published works [4] did not efficiently include all tradeoffs, such as comparison of bit error rate (BER), modulation level, channel capacity, and complexity. In fact, even if several technical papers have already discussed this issue, they mainly investigated the modulation performance for specific applications or system requirements and thus, to the best of our knowledge, did not cover the whole comparison spectrum [5].

The objective of this paper is indeed to evaluate all these parameters and their impact on each scheme performance. For this aim, we considered the PPM in time-hopping mode (TH-mode), the OOK in direct-sequence mode (DS-mode), and the binary PAM (BPAM) in both TH- and DS-modes. The channel model is the UWB IEEE 802.15.3a indoor channel model under additive white Gaussian noise (AWGN) [6]. Note that the white noise channel model is largely used in the literature due to its relative simplicity. Because the target here is to compare the performance of different UWB pulse modulation schemes under the same channel model, a relatively simple model can be the best candidate. Note also that this channel model can be specified for different propagation scenarios, such as extremely indoor non-line-of-sight (ENLOS) or outdoor line-of-sight (LOS). In this work, we focused on the indoor propagation channel model to take advantage of UWB frequency selective fading.

Also, the transmit power was evaluated by integrating the fifth derivative of the power spectrum density (PSD) of the Gaussian pulse over the whole bandwidth.

2. Modulation Schemes

2.1. M-PAM. In pulse-amplitude modulation, the same waveform is sent with different amplitudes corresponding to different data being transmitted. The BPAM can be presented using antipodal, monocyclic, or Gaussian pulses. The transmitted signal for M-PAM can be expressed as [7]

$$S_{\mathrm{PAM}}(t) = \sum_{j=-\infty}^{\infty} \sum_{m=1}^{M} \delta_m(j) d_m P(t - jT_s), \tag{1}$$

where $\delta(j) = [\delta_1(j), \delta_2(j) \ldots, \delta_M(j)]$ is an indicator transmitter pulse vector, that is, for each known unit impulse j, only one element of the vector is equal to unity otherwise zero; T_s is the pulse symbol period, M is the modulation level, and P is the pulse shape impulse response. For multiuser case, d_m is the amplitude of independent and identically distributed (IID) random signals according to an equiprobable distribution. The related PSD can be formulated as [4]

$$S_{\mathrm{PAM}}(f) = S_{\mathrm{CPAM}}(f) + S_{\mathrm{dPAM}}(f), \tag{2}$$

where $S_{\mathrm{CPAM}}(f)$ and $S_{\mathrm{dPAM}}(f)$ are, respectively, the desired continuous part (nonperiodic) and the undesired discrete part (periodic), which induces more spectral lines and lower mutual information [4]. For real data with equal probability of occurrence, $S_{\mathrm{PAM}}(f)$ becomes [6, 7]

$$S_{\mathrm{PAM}}(f) = \frac{\sigma_d^2}{T_s} |P(f)|^2 + \frac{\mu_d^2}{T_s^2} \sum_{j=-\infty}^{\infty} \left| P\left(\frac{j}{T_s}\right) \right|^2 \delta\left(f - \frac{j}{T_s}\right), \tag{3}$$

where σ_d^2 and μ_d are the variance and mean of the random data sequence, respectively. In case of repetition pulse coding [6, 8], each random data contain number of pulses with various amplitude (PAM case) that indicate just one bit of data. Let us consider the symbol period limited by trade of data rate and pulse numbers. For instance, for wider T_s, the data rate is indeed lower but does have better performance with higher pulse repetition coding (increasing pulse numbers), and inversely. On the other hand, if a time-hopping PAM (TH-PAM) is considered, they are dependent on frequency, which is not the case in this study.

In narrowband, using a filter bank receiver or a mixer bank receiver can mitigate the narrowband interference while splitting the UWB bandwidth to the narrowband. Thus, the average power or variance of the UWB signals can be calculated by integrating the PSD in frequency domain [9, 10]

$$\begin{aligned} \mathrm{Var}(S_{\mathrm{PAM}}(t)) &= \int_{-\infty}^{+\infty} S_{\mathrm{PAM}}(f)\, df \\ &= \int_{-\infty}^{+\infty} \left[\frac{\sigma_d^2}{T_s} |P(f)|^2 \right. \\ &\qquad \left. + \frac{\mu_d^2}{T_s^2} \sum_{j=-\infty}^{\infty} \left| P\left(\frac{j}{T_s}\right) \right|^2 \delta\left(f - \frac{j}{T_s}\right) \right] df \\ &= \frac{\sigma_d^2}{T_s} \int_{-\infty}^{+\infty} |P(f)|^2 df \\ &\quad + \frac{\mu_d^2}{T_s^2} \sum_{j=-\infty}^{\infty} \left| P\left(\frac{j}{T_s}\right) \right|^2. \end{aligned} \tag{4}$$

Assuming the carrier frequency of the receiver is f_{c0} and the bandwidth of the bandpass filter is B, the UWB interference power can be expressed as [10]

$$\begin{aligned} P_I &= \frac{\sigma_d^2}{T_s} \int_{-\infty}^{+\infty} |P(f) H_T(f)|^2 df \\ &\quad + \frac{\mu_d^2}{T_s^2} \sum_{(j/T) \pm f_{c0} \in [-B/2 \;\; B/2]} \left| P\left(\frac{j}{T_s}\right) H_T\left(\frac{j}{T_s}\right) \right|^2, \end{aligned} \tag{5}$$

with $H_T(f) = H_{\mathrm{ch}}(f) H_B(f)$, where $H_B(f)$ and $H_{\mathrm{ch}}(f)$ are the Fourier transform for the filter and the channel impulse response, respectively. For an ideal bandpass filter, the above equation can be formulated as [10]

$$\begin{aligned} P_I &= \frac{2\sigma_d^2}{T_s} \int_{f_{c0}-(B/2)}^{f_{c0}+(B/2)} |P(f)|^2 df \\ &\quad + \frac{2\mu_d^2}{T_s^2} \sum_{(j/T) + f_{c0} \in [-B/2 \;\; B/2]} \left| P\left(\frac{j}{T_s}\right) \right|^2. \end{aligned} \tag{6}$$

Therefore, interference power can be affected by the following factors.

(i) The symbol period ($1/T_s$); in fact, increasing T_s will both increase the pulse repetition frequency and decrease the energy spectral density, while the corresponding continuous component of the power spectral density remains unchanged. So the pulse repetition leads to a discrete line spectrum. The line spectral density is composed of the delta function and separated by the pulse repetition frequency.

(ii) The energy spectral density (ESD) of the pulse waveform, $|P(f)|^2$.

(iii) The power spectral density (PSD) of the UWB chip sequence $S_{\mathrm{PAM}}(f)$ determined by σ_d^2 and μ_d for real and mutually uncorrelated sequences. Therefore, a proper pseudorandom (PR) code, directly related to the pulse repetition frequency and corresponding

PSD, could be selected to reduce the discrete spectral components. If the mean μ_d is not zero, discrete components (spectral lines) will appear in $S_{\text{PAM}}(f)$. However, for a sequence of ± 1, these components will disappear. On the other hand, if the UWB pulse train is modulated by an all "one" sequence ($\sigma_d^2 = 0$, $\mu_d = 1$), the PSD of $S_{\text{PAM}}(f)$ will be composed only of discrete components. Thus, if these components, which generally have a stronger PSD than continuous ones [2, 5], are in the band of narrowband systems, they will have a bigger effect on the performance of the victim receiver.

An alternative is to send alternating positive and negative pulses [2, 9]. This line coding scheme is often called alternate mark inversion (AMI). Following [10], it has been demonstrated that with equal probable binary elements, the PSD is given by

$$S_{\text{AMI}}(f) = \frac{1}{2T_s} |P(f)|^2 [1 - \cos(2\pi f T_s)], \tag{7}$$

which shows there are no spectral lines, and thus, the bipolar PAM signal has a lower bit error rate compared to the nonbipolar PAM signal, which suffers from the presence of more spectral lines (Figure 1).

2.2. OOK. Compared to others, OOK can be seen as the simplest scheme. In this technique, sending a pulse corresponds to bit "1" and no pulse means "0". Therefore, because of the equal probability of either symbols, $\sigma_d^2 = 0.25$, $\mu_d = 0.5$, and the PSD becomes [6, 10]

$$S_{\text{OOK}}(f) = \frac{1}{4T_s} |P(f)|^2 + \frac{1}{4T_s^2} \sum_{j=-\infty}^{\infty} \left| P\left(\frac{j}{T_s}\right) \right|^2 \delta\left(f - \frac{j}{T_s}\right). \tag{8}$$

In a variant (antipodal signals), the transmitter sends a pulse of duration T_p much higher than the bit time T_b to indicate bit "1" and the negative of this pulse for "0". Therefore, with equiprobable elements, we have $\sigma_d^2 = 1$, $\mu_d = 0$ and thus, a PSD of [10]

$$S_{\text{ant}}(f) = \frac{1}{T_s} |P(f)|^2, \tag{9}$$

showing that the PSD of antipodal does not have any spectral lines or discrete components. Note that OOK and binary-PPM are similar. Therefore, only 2-PPM performance was evaluated to avoid duplication.

2.3. M-PPM. In PPM, the chosen bit to be transmitted influences the position of the UWB pulses. The signal at the output of the transmitter cascade, $s(t)$, can be expressed as [1, 2, 6]:

$$S_{\text{PPM}}(t) = \sum_{j=-\infty}^{\infty} \sum_{m=1}^{M} P(t - jT_s - c_m T_C - a_m \varepsilon), \tag{10}$$

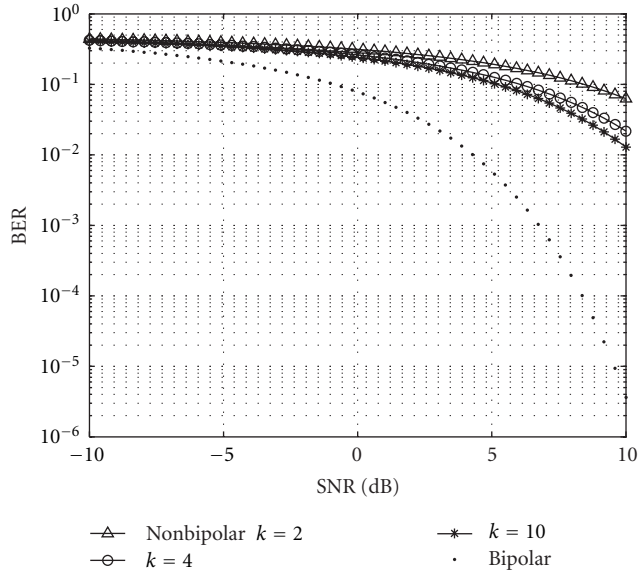

Figure 1: BER AWGN channel comparison with various polarization k.

where j is the number of transmitted bits, T_s is the symbol period, c_m is the time-hopping code, $c_m T_c$ is the pseudorandom code in chip duration T_C, a_m depends on j, and ε is the time shift associated with TH-PPM.

The chip time interval T_C represents only one pulse in the time frame period. Note that $a_m \varepsilon + T_p < T_c$ with T_p the pulse period.

The Fourier transform of the PSD of M-PAM can be expressed as [11]

$$S_{\text{PPM}}(f) = \int_{-\infty}^{+\infty} S_{\text{PPM}}(t) e^{-j2\pi f t} dt. \tag{11}$$

Leading to the following PSD, expressed in terms of continuous and discrete parts

$$PS_{\text{PPM}}(f) = PS_{\text{CPPM}}(f) + PS_{\text{dPPM}}(f) \tag{12}$$

with

$$PS_{\text{CPPM}}(f) = \frac{|P(f)|^2}{T_s} \left[1 - \left(\frac{1}{M} \frac{\sin(\pi f T)}{\sin(\pi f T/M)} \right)^2 \right]$$

$$PS_{\text{dPPM}}(f) = \frac{|P(f)|^2}{T_s^2} \left(\frac{1}{M} \frac{\sin(\pi f T)}{\sin(\pi f T/M)} \right)^2 \times \left[\sum_{j=-\infty}^{\infty} \delta\left(f - \frac{j}{T_s}\right) \right], \tag{13}$$

which can be simplified to [6, 11]

$$PS_{\text{PPM}}(t) = \frac{1}{T_s^2} \sum_{j=-\infty}^{\infty} \sum_{m=1}^{M} \left| P\left(\frac{jM}{T_s}\right) \right|^2 \delta\left(f - \frac{jM}{T_s}\right), \tag{14}$$

showing a smother PSD than of PAM, leading to less narrowband interference. The single pulse of the UWB signal is

placed into one of $N = T_{\text{sym}}/T_h$ slots, where N is the number of slots per symbol, T_h is the pulse width and T_{sym} is the symbol time. The number of bits per one PPM symbol is equal to $\log_2^N$.

Note that by increasing M (modulation level) the data rate will increase as well. Furthermore, the average transmitted power will be increased by a factor of M.

In this case, the N slots are divided into L groups. Each group includes N/L slots with a single pulse. With this, the average bit number will be [11]

$$N_b' = \log_2^{(N/L)^L} = L\left(\log_2^N - \log_2^L\right) \quad N >> L,$$
$$N_b' = L\log_2^N = N_b. \tag{15}$$

Thus, modifying the bit rate can improve the throughput of number of pulses per N slots, but it will raise other issues.

(i) A larger bandwidth requirement, as the number of pulses per symbol interval increases.

(ii) The pulse width relaxation will be limited.

(iii) All symbols can be orthogonal. To solve this for large N, one can use predefined pulse arrangement such that no pulse is put in the same position. In other words, to avoid pulse interpath interference (IPI) or pulse jamming, we should decrease the pulse period or increase the chip period.

Note that more information on PSK modulation can be found in [4, 6]. Because of its complexity, it has been introduced here just for comparison.

3. AWGN Channels

Under AWGN UWB channel models expressed by the IEEE 802.15.3a standard, symbol, or bit error rates can be easily expressed, leading to an optimum receiver [6, 7], consisting on an optimum demodulator (coherent demodulator). First, let us assume a zero system margin (no power loss between equipment connections), that is, $M_s = 0$.

For any binary modulation, the BER can be calculated using the distance between two symbols as [6]

$$P_b = Q\left(\sqrt{\frac{d}{2N_0}}\right). \tag{16}$$

This distance is different for each modulation scheme

$$d_{\text{PPM}} = \sqrt{2\gamma_b}; \qquad d_{\text{PSK}} = 2\sqrt{\gamma_b};$$
$$d_{\text{OOK}} = \sqrt{2\gamma_b}; \qquad d_{\text{PAM}} < \sqrt{2\gamma_b}, \tag{17}$$

$\gamma_b = E_{\text{Rx}}/N_0 = N_s\gamma_p$ is the average bit energy in the receiver and γ_p is its average pulse energy. Table 1 summarizes the BER and SER performance for different modulation schemes.

For simplicity, let us assume $N_s = 1$ with a normalized pulse energy. From theory, and as shown in Figure 2, binary PAM has 3 dB more power efficiency than PPM. As M is increasing, the performance of M-PPM also increases. This is due to space dimensionality that makes more noise orthogonal and causes the elements of the covariance noise matrix, Q_c, to be almost zero [9, 12]. Since the signal-to-noise ratio (SNR) is given by $\text{SNR}_r = S^T Q_c^{-1} S$, it will also increase. Also, M-PPM requires lower transmission power in high modulation levels. On the other hand, the performance of M-PAM becomes worse due to decreased symbol distance and as a result, $|Q_c|$ will increase leading to more interference at narrowband. Thus, by increasing the modulation level, the M-PPM will exhibit better performance.

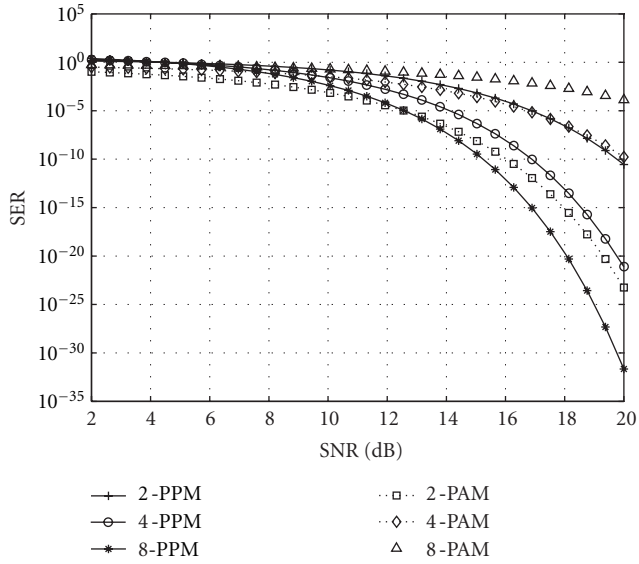

Figure 2: Symbol error rate for different M levels of M-PAM and M-PPM ($N_s = 1$).

Note that (17) confirms what was mentioned above, that is, simulating 2-PPM and OOK parameters leads to similar performance. Therefore, we just simulated and compared the M-PAM and the M-PPM in terms of BER versus SNR while a comparison between OOK and PPM is not necessary.

Table 2 summarizes the comparison between the different modulations schemes in terms of noise interference, spectral lines, transceiver complexity, pulse energy variance, and bandwidths.

As shown, the candidate pulse modulation is strongly related to the application. In fact, if simplicity is considered, the repeat pulse coding or OOK modulation will be the good option but in case of NBI the 4-PPM should be chosen to satisfy all spectrum requirements.

4. Data Rate and Maximum Distance

To further investigate the modulation scheme performance, let us assume that the signal propagation occurs over free space. Thus, the free-space attenuation A_m can be expressed as [6, 13]

$$A_m = \frac{4\pi D^2 L}{G_T S_R}, \tag{18}$$

Table 1: BER and SER in AWGN channel for different UWB modulations.

TH-BPPM	Orthogonal single pulse ($N_s = 1$) $P_{rb} = Q\left(\sqrt{N_s\gamma_b}\right), Q(x) = \frac{1}{2}\operatorname{erfc}\left(\frac{x}{\sqrt{2}}\right)$ $s_m = \begin{cases} s_0 = +\sqrt{p_{Tx}}[1 - R_0(m)], \\ s_1 = -\sqrt{p_{Tx}}[1 - R_0(m)] \end{cases}$ where $R_j(\varepsilon)$ is autocorrelation of the pulse S_m. orthogonal multipulse signal with TH coding: $P_{rb} = Q\left(\sqrt{N_s\gamma_b(1 - R_0(m))}\right)$
BPAM/BPSK	$P_b = Q(\sqrt{2\gamma_b})$
M-PPM	$P_M = \frac{1}{\sqrt{2\pi}}\int_{-\infty}^{\infty}\left[1 - \left(\frac{1}{\sqrt{2\pi}}\int_{-\infty}^{y} e^{-x^2/2}dx\right)^{M-1}\right]\cdots$ $\cdots \exp\left[\frac{-1}{2}\left(y - \sqrt{2\gamma_s}\right)^2\right]dy$ $P_b = \frac{2^{k-1}}{2^k - 1}P_M \approx \frac{1}{2}P_M$
M-PAM	$P_M = \frac{2(M-1)}{M}Q\left(\sqrt{\frac{6\log_2(M)\gamma_b}{M^2 - 1}}\right) \quad P_b = \frac{1}{k}P_M$ $\gamma_s = \log_2(M)\gamma_b \quad \gamma_b = N_s\frac{\xi_b}{N_0}$

Table 2: Comparison of various pulse modulation techniques in terms of bandwidth, spectral line, noise sensitivity, transceiver complexity, and pulse energy variance.

	Bandwidth requirement (normalized)	Power requirement (normalized)	Noise sensitively	Spectral line power distortion	Transceiver complexity	Pulse energy variance
PAM	1	1	Highest (1 dimension)	Yes	Low	$\left(\frac{M^2 - 1}{6}\right)\frac{1}{\gamma_s}$
PPM	$\left(\frac{M}{\log_2 M}\right)\left(\frac{\tau}{T_s}\right)$	$\sqrt{\frac{2}{M\log_2 M}}$	Lowest (M dimensions)	Yes (lower)	Highest (by M)	$\frac{1}{\gamma_s}$
OOK	1	1	Very high	Yes (high)	Lowest	$\frac{1}{\gamma_s}$
BPSK	$\frac{\tau}{T_s}$	1.12	Lower ($M/2$ dimensions)	No	High (by $M/2$)	$\frac{1}{\gamma_s}$

with D is the distance of propagation, S_R is the antenna effective area, L is the system hardware loss, and G_T is the transmitter antenna gain. In this work, we assumed $L = 1$ (no losses in the system hardware). The pulse waveform is the 5th derivative of a monocyclic Gaussian pulse and its PSD is given by [13]

$$P_s(f) = A_{\max}\frac{(2\pi f\delta)^{2n}e^{-(2\pi f\delta)^2}}{n^n e^{-n}}; \qquad A_m = 10^{-13.125}; \quad \delta = 51\,\text{ps}, \tag{19}$$

leading to the following receiving signal power

$$P_r = \frac{M_s \text{SNR}_{\text{spec}} N_0}{2}, \tag{20}$$

where N_0 is the thermal noise power, SNR_{spec} is the system requirement SNR, and $H(f)$ is the frequency response of the indoor channel, which can be expressed as [13]

$$|H(f)| = \sqrt{\frac{1}{A_m(f)}R(f)}, \tag{21}$$

where $R(f)$ is the shadowing parameter that depends on the geography of the propagating environment (usually assumed to be 6 dB). The system margin M_s is assumed to be 1 dB. From this, the distance can be reformulated as [6, 7]

$$D^2 = \frac{\left(G_T G_R c^2/(4\pi)^2 R_b\right) 2\int_{fL}^{fH}(P_s(f)/f^2)df}{M_s \text{SNR}_{\text{spec}}(1/2)N_0}, \qquad N_0 = kT_s(f) = k(T_A + (F(f) - 1)T_0), \tag{22}$$

where T_s is the noise temperature at the receiver, T_A is the receiver antenna temperature, T_0 is the room temperature (usually $T_0 = 300°K$), k is the Boltzmann constant, $F(f)$ is the noise factor of the receiving device, and R_b is the data rate. Given a specific SNR (i.e., the SER of a specific modulation scheme), one can evaluate the maximum transmit distance. Figure 3 shows the maximum distance as function of data rate for PAM and PPM modulation schemes. The following assumptions have been made

(i) SER is lower than $10^{-5}(N_s = 1,\ T_s = 3ns)$.

(ii) No fading margin required and PSD of noise is constant (E_b/N_0).

It is observed that BPAM (BPSK) has the best data rate over short distances with respect to complexity. However, by increasing the modulation level M, the M-PPM data rate can be improved ($\text{SER}_{8\,\text{PPM}} < \text{SER}_{4\,\text{PPM}} < \text{SER}_{2\,\text{PPM}}$) while the opposite occurs for M-PAM.

5. Channel Capacity

A channel with M-ary PPM/PAM modulation has discrete-valued inputs and continuous-valued outputs, which imposes an additional capacity calculation. Let s_m be the encoded M-ary PPM/PAM signal vector input to the channel

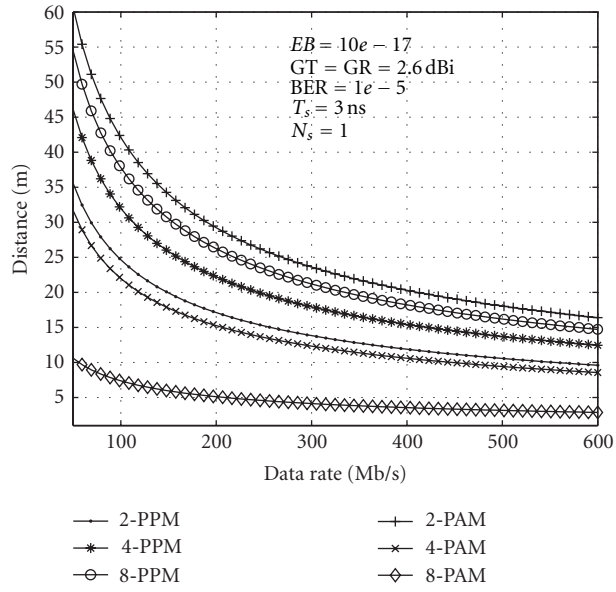

Figure 3: M-PAM and M-PPM signals data rate for short distances and uncoded systems.

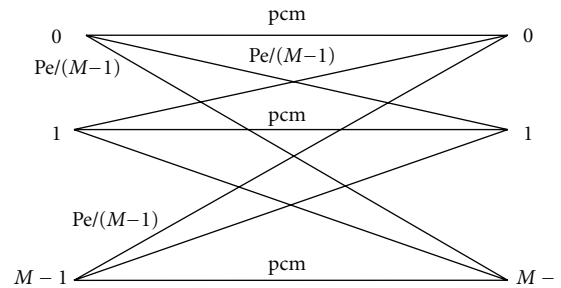

Figure 4: Channel capacity model for M-ary.

and r_i the ith diversity channel output vector corrupted by the AWGN noise vector. Let w_i be an M-dimensional Gaussian vector with zero mean and variance $\sigma_w^2 = N_0/2$ along each real direction (multipath). This output vector is given by:

$$r_i = s_m + w_i \quad 1 \le i \le L, \tag{23}$$

where L is the number of multipaths. The channel capacity (bits/channel), with input signals restricted to an equiprobable M-ary signal constellation and with no restrictions on the channel output, can be written as [14]

$$C = \log_2(M) - \frac{1}{M}\sum_{m=1}^{M}\int P\left(\frac{r}{s_m}\right)\log_2\left(\frac{\sum_{k=1}^{M}P(r/s_k)}{P(r/s_m)}\right)dy, \qquad P\left(\frac{r}{s_m}\right) = \prod_{i=1}^{L}\left[\left(\frac{1}{\pi N_0}\right)e^{\left(-(ri-\sqrt{E})^2/N_0\right)}\right], \tag{24}$$

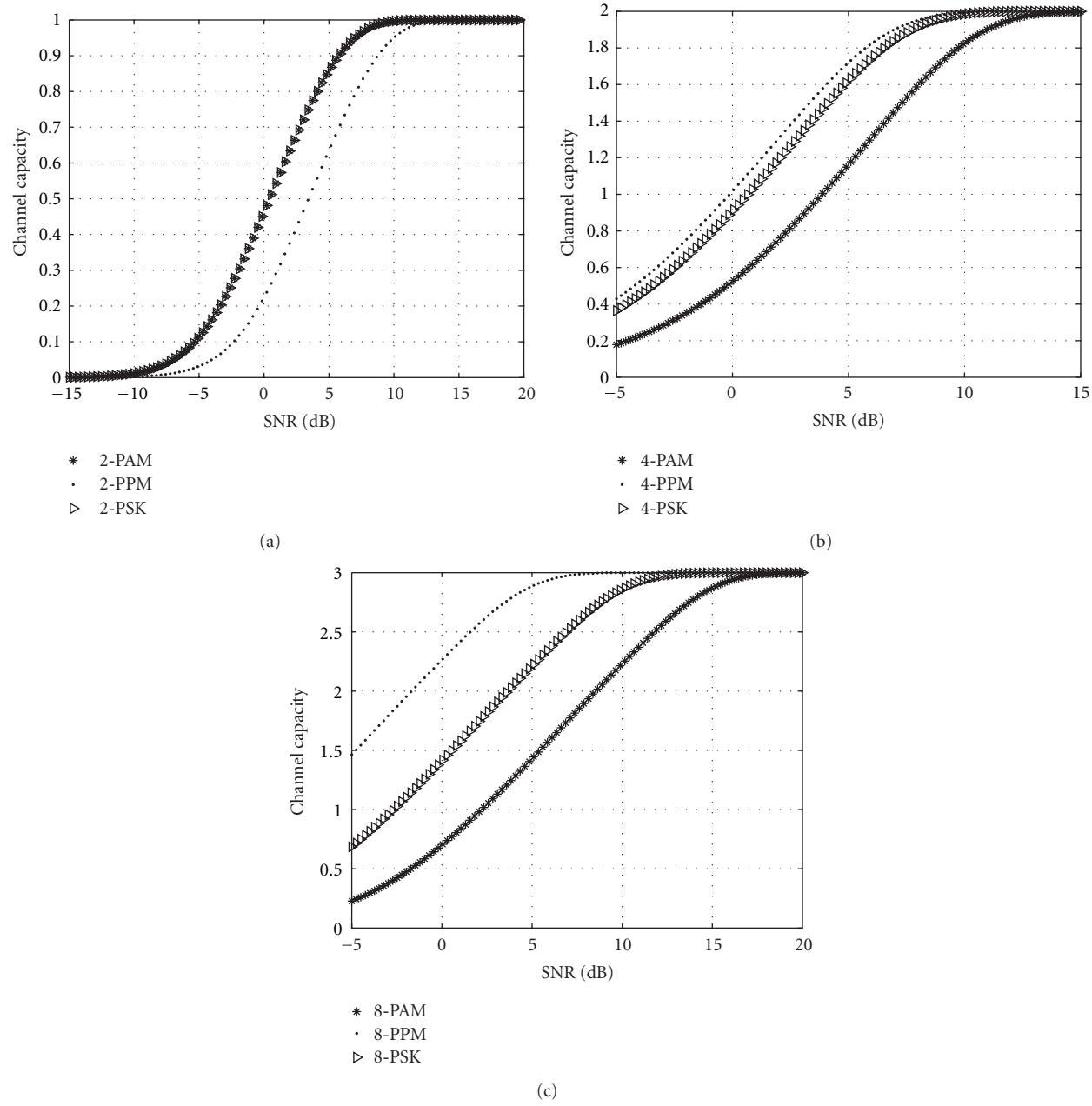

Figure 5: Channel capacity comparison of PAM, PPM, and PSK in various modulation levels.

with P is the probability to receive a signal from the transmitter and N_0 is the PSD of white noise. For M-PAM over an AWGN channel, we obtain

$$C = \log_2(M) - \frac{1}{M}\sum_{k=0}^{M-1} \times \left\langle \left\{ \log_2 \sum_{p=0}^{M-1} \exp\left(\sum_{i=1}^{L} \frac{|w_i|^2 - \left| s_k + w_i - s_p \right|^2}{N_0} \right) \right\} \right\rangle, \tag{25}$$

where s_p is one of the M-ary PAM signals. For M-PPM, the probability of receiving a signal is [7, 9, 14]

$$P\left(\frac{r}{s_m}\right) = \prod_{i=1}^{L} \left[\left(\frac{1}{\pi N_0}\right)^{M/2} \left(\prod_{j=1}^{M} e^{-r_{ij}^2/2{\sigma_T}^2} \right) e^{-\left(r_{ij} - \sqrt{E_g}\right)^2/N_0} \right]$$

$$r_{ij} = \sqrt{E_g} + w_{ij},$$

$${\sigma_T}^2(n) = {\sigma_{\text{pre}}}^2(n) + {\sigma_{\text{post}}}^2(n) + {\sigma_w}^2,$$

$$\sigma^2_{\text{pre}}(n) = \frac{1}{N}\sum_{k=-\infty}^{-1} h^2(n-k),$$

$$\sigma^2_{\text{post}}(n) = \frac{1}{N}\sum_{k=1}^{n} h^2(n-k) \quad \text{for } n > 0, \tag{26}$$

where σ_T^2 is the total noise variance, E_g is the signal energy, M is the signal dimension, $\sigma^2_{\text{pre}}(n)$ is the variance of the noise pulses preceding the present signal pulse at time n, $\sigma^2_{\text{post}}(n)$ is the variance of the noise of the pulses following the present signal, and $h(n)$ is the discrete channel response.

Giving the following channel capacity model for symmetric channel (Figure 4), and [9, 12, 15]

$$C_{M\text{-PPM}} = \frac{1}{M}\sum_{i=0}^{M-1}\sum_{j=0,\, j\neq i}^{M-1}\frac{P_e}{M-1}\log\left[\frac{(P_e/(M-1))}{(1/M)}\right] + \frac{1}{M}\sum_{i=0}^{M-1}\sum_{j=0,\, j\neq 0}^{M-1} P_{\text{cm}}\log\left[\frac{P_{cm}}{(1/M)}\right], \tag{27}$$

$$C_{M\text{-PPM}} = \log_2(M) + P_{\text{cm}}\log_2(P_{\text{cm}}) + (1-P_{\text{cm}})\log_2\left(\frac{1-P_{\text{cm}}}{M-1}\right).$$

Figure 5 shows the channel capacity of various modulation schemes. In this figure, the capacity can be improved by increasing the modulation level for M-PPM, M-PAM, and M-PSK. Note that the theory details about this comparison are expressed in Table 2.

6. Maximum Transfer Power

From a communication theory perspective, the most important characteristic of UWB systems is the power-limited regime operation. Following standards and regulations, there is a maximum allowed transmit power P_t. This limitation has a direct impact on the maximum transmit distance and data rate [8, 16]

$$\frac{P_t}{P_r}(\text{dB}) = C_0 + 10\chi\log_{10}\left(\frac{\lambda}{4\pi d}\right) + X_R(\text{dB}), \tag{28}$$

where

$$P_t(\text{dB}) = 10\log_{10}\left(\frac{M_s\ R_b\ E_b^0}{G_T\ G_R}\left(\frac{4\pi}{\lambda}\right)d^2\right). \tag{29}$$

In the above equations, X_R is the average shadowing system, χ is the path-loss component, and C_0 is the maximum UWB pulse power, assumed to be -41.42 dBm [8]. E_b^0 is the energy per bit ($1.82.\ 10^{-19}$ W) for a specified BER of 5.10^{-5}.

In Figure 6, we compared the transfer power for different modulation levels at a fixed data rate (200 MHz) and as function of maximum transmitter power and distance. It can be seen that BPSK soft decision has a higher maximum distance compared to other modulation schemes.

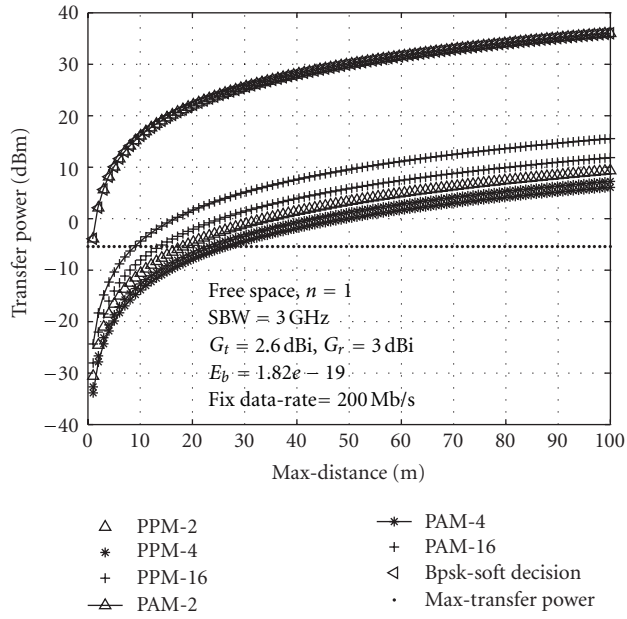

Figure 6: Maximum transfer power for M-PAM-M-PPM, BPSK for a fixed data rate of 200 Mb/s. The horizontal line (close to -5 dBm) represents the maximum transmit power specified by FCC regulations.

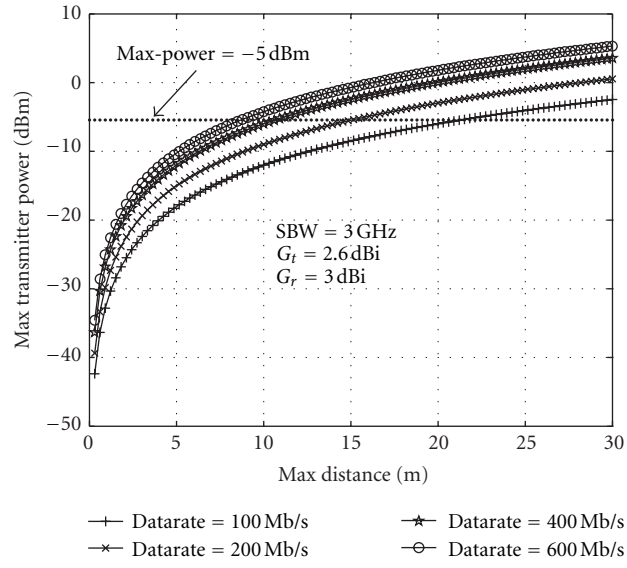

Figure 7: Maximum transfer power for 4-PPM with various data rate. The horizontal line (close to -5 dBm) represents the maximum transmit power specified by FCC regulations.

By increasing the modulation level M, M-PPM will be improved but M-PAM and M-PSK will exhibit a lower performance, due to more noise interference (noise dimensionality). Then again M-PPM has better narrowband interference robustness in terms of required less transmit power with respect to system complexity. Furthermore, the 4-PPM has an optimum modulation level which covers all tradeoff as sorted by Table 2.

In Figure 7, we compared the 4-PPM in various data rates using the same transmitter and channel propagation scenario

as in Figure 5 for different modulation levels. As expected, by increasing distance, the data rate will decrease, requiring higher transmitter power. For short distance applications (<10 m), the data rate cannot exceed 200 Mb/s even with an LOS scenario and AWGN channel assumption. This demonstrated that UWB technology cannot practically provide the expected high data rate (>400–600 Mb/s) unless a pulse coding is considered. In fact, with more complexity and higher modulation levels, the data rate can be significantly improved but with the cost of higher transmitter power.

7. Conclusion

Various UWB pulse modulation schemes were evaluated in this paper and their performance was compared in terms of narrowband interference robustness, symbol error rate, system complexity, data rate, and maximum transmit power with respect to transceiver distance and channel capacity.

It appears that BPAM has the highest data rate in terms of maximum distance and transmit power. However, M-PPM has better power efficiency and channel capacity, at the expense of increased complexity and bandwidth.

If bandwidth is not an issue, the M-PPM is the best option, due to lower spectral lines (smoother PSD), higher dimensionality (orthogonally of noise), and narrowband interference robustness. However, if the UWB receiver is single band, the M-PPM is not the optimum option in terms of bandwidth.

If the system complexity and bandwidth are the limiting factors, OOK is the best choice, but has more spectral lines and higher probability of error which leads to higher risk of interference. Finally, because of signal orthogonally and lower spectral lines (smoother PSD), the 4-PPM (optimum modulation level) can be the best candidate for NBI robustness and can be used for unique UWB rake filter-bank receiver design.

References

[1] A. Naanaa and S. Belghith, "Performance enhancement of a time hopping—pulse position modulation ultra-wideband system using guided local search," *IET Journal of Communications*, vol. 5, no. 15, pp. 2212–2220, 2011.

[2] Q. Zhu, Z. Jia, and C. Zou, "On the performance of different modulation schemes for UWB systems in a multipath channel," in *Proceedings of the IET International Conference on Wireless, Mobile and Multimedia Networks*, pp. 1–4, November 2006.

[3] R. Hidayat and Y. Miyanaga, "IR-UWB pulse position modulation and pulse shape modulation through S-V channel model," in *Proceedings of the 2nd International Conference on Communication Software and Networks (ICCSN '10)*, pp. 214–217, February 2010.

[4] A. Al Zaman and N. Islam, "Modulation schemes and pulse shaping in ultra wideband," in *Proceedings of the IEEE Southeast conference*, pp. 142–146, April 2008.

[5] C. Ngo and D. Birru, "Analysis of UWB modulation techniques," in *Proceedings of the International Conference on Wireless Networks (ICWN '03)*, pp. 646–652, June 2003.

[6] M. G. Di Benedetto and G. Giancola, *Understanding Ultra Wide Band Radio Fundamentals*, Prentice Hall, New York, NY, USA, 2004.

[7] M. Ghavami, L. B. Michael, R. Kohno, and U. W. B. Signals a, *Systems in Communication Engineering*, John Wiley & Sons, New York, NY, USA, 2nd edition, 2007.

[8] H. Sheng, "On the spectral and power requirements for ultra-wideband transmission," in *Proceedings of the International Conference on Communications (ICC '03)*, pp. 738–742, May 2003.

[9] L. Ma and T. C. Wang, "Performance analysis and simulations of UWB-PAM communications in AWGN channel," in *Proceedings of the 4th International Conference on Microwave and Millimeter Wave Technology (ICMMT '04)*, pp. 830–833, August 2004.

[10] Z. Ye, "Power spectral density and in-band interference power of UWB signals at narrowband systems," in *Proceedings of the IEEE International Conference on Communications*, pp. 3561–3565, June 2004.

[11] J. Nielsen and S. Zwierzchowski, "Power spectral density of a UWB signal with discrete quantized pulse positions," *Canadian Journal of Electrical and Computer Engineering*, vol. 28, no. 3-4, pp. 145–154, 2003.

[12] P. E. McIllree, "Calculation of channel capacity for M-ary digital modulation signal sets," in *Proceedings of the IEEE Singapore International Conference on Networks*, pp. 639–643, Singapore, September 1993.

[13] S. S. Mo, "On the power spectral density of UWB signals in IEEE 802.15.3a," in *Proceedings of the IEEE Wireless Communications and Networking Conference (WCNC '04)*, pp. 999–1003, March 2004.

[14] L. Zhao and A. M. Haimovich, "Capacity of M-ary PPM ultra-wideband communications over AWGN channels," in *Proceedings of the IEEE 54th Vehicular Technology Conference (VTC FALL '01)*, pp. 1191–1195, October 2001.

[15] R. Pasand, "Capacity of PPM ultra-wideband communications with inter pulse interference," in *Proceedings of the Canadian Conference on Electrical and Computer Engineering*, pp. 2355–2358, May 2004.

[16] V. Somayazulu, J. R. Foerster, and S. Roy, "Design challenges for very high data rate UWB systems," in *Proceedings of the 36th Asilomar Conference on Signals Systems and Computers*, pp. 717–721, November 2002.